even with modest finesse $F = 100$, the resolution (see Eq. (4.62)) is $\Delta\nu = 30$ MHz. Thus for $\lambda = 500$ nm, namely $\nu = 6 \times 10^{14}$ Hz

$$\frac{\nu}{\Delta\nu} = 2 \times 10^7.$$

In the following two sections the Zeeman effect and the theory of hyperfine structure are discussed in some detail. We also discuss the isotope shift and present data on the shift between the spectral lines of hydrogen and deuterium. We then describe a measurement of the Zeeman splitting of the 546.1-nm green line of Hg, using a Fabry–Perot etalon. The final section is devoted to a measurement of the hyperfine structure of rubidium using Doppler-free saturation spectroscopy.

The bibliography on atomic spectroscopy is vast and because of the "reach" of laser experiments it is kept up-to-date. A list of suggested references is given at the end of the chapter.

6.2. THE ZEEMAN EFFECT

6.2.1. The Normal Zeeman Effect

As already discussed in Section 1.4, the solution of the Schrödinger equation[3] yields "stationary states" labeled by three integer indices, n, l, and m, where $l < n$ and $m = -l, -l+1, \ldots, l-1, l$. For the screened Coulomb potential, the energy of these states depends on n and l but not on m; we therefore say that the $(2l+1)$ states with the same n and l index are "degenerate" in the m quantum number. Classically we can attribute this degeneracy to the fact that the plane of the "orbit" of the electron may be oriented in any direction without affecting the energy of the state, since the potential is spherically symmetric.

If a magnetic field B is switched on in the region of the atom, we should expect that the electrons (and the nucleus[4]) will interact with it. We need only consider the electrons *outside* closed shells, and assume there is one such electron; indeed the interaction of the magnetic field with this electron

[3]"Quantum Mechanics" A. Das and A. Melissinos, Gordon and Breach (1986), New York. Or any other text on quantum mechanics.

[4]For our present discussion this interaction of the nucleus with the external field is so small that we will neglect it.

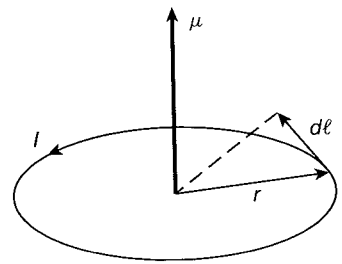

FIGURE 6.1 Magnetic moment due to a current circulating in a closed loop.

yields for each state an additional energy ΔE, given by

$$\Delta E = m\mu_B B. \tag{6.5}$$

Thus, the total energy of a state depends now on n, l, and m, and the degeneracy has been removed.

To see how this additional energy arises we consider the classical analogy. See Fig. 6.1. The orbiting electron is equivalent to a current density[5]

$$\mathbf{J}(\mathbf{x}) = -e\mathbf{v}\delta(\mathbf{x} - \mathbf{r}),$$

where $\mathbf{r}$ is the equation of the orbit and $\mathbf{x}$ gives the position of the electron; the negative sign arises from the negative charge of the electron. Such a current density gives rise to a magnetic-dipole moment

$$\boldsymbol{\mu} = \frac{1}{2}\int \mathbf{x} \times \mathbf{J}(\mathbf{x})\, d^3x = -\frac{1}{2}\, e(\mathbf{r} \times \mathbf{v}).$$

[5]For a circular orbit, the electron is equivalent to a current $I = \Delta Q/\Delta T = e/T = e\omega/2\pi$, where ω is the angular frequency $\omega = v/a$; a is the radius of the orbit. However, a plane closed loop of current gives rise to a magnetic moment $\mu = IA$, where A is the area enclosed by the loop; in our case $A = \pi a^2$, hence

$$\mu = \frac{ev}{2\pi a}\,\pi a^2 = \frac{eva}{2}.$$

The angular momentum for the circular orbit is $L = m_e va$, hence

$$\mu = \frac{e}{2m_e}L$$

as in Eq. (6.1).

However, the angular momentum of the orbit is given by

$$\mathbf{L} = \mathbf{r} \times \mathbf{p} = m_e(\mathbf{r} \times \mathbf{v}),$$

so that

$$\boldsymbol{\mu} = -\frac{e}{2m_e}\mathbf{L} = -\frac{e\hbar}{2m_e} l\mathbf{u}_L, \tag{6.6}$$

where we expressed the angular momentum of the electron in terms of its quantized value $\mathbf{L} = l(h/2\pi)\mathbf{u}_L$ and $\mathbf{u}_L$ is a unit vector along the direction of $\mathbf{L}$. The energy of a magnetic dipole in a homogeneous field is

$$E = -\boldsymbol{\mu} \cdot \mathbf{B} = \frac{e}{2m_e}\mathbf{L} \cdot \mathbf{B}, \tag{6.7}$$

but the angle between $\mathbf{L}$ and the external field $\mathbf{B}$ cannot take all possible values.[6] We know that it is quantized, so that the projection of $\mathbf{L}$ on the z axis (which we can take to coincide with the direction of $\mathbf{B}$ since no other preferred direction exists) can only take the values $m = -l, -l+1, \ldots, l-1, l$. Thus the energy of a particular state n, l, m in the presence of a magnetic field will be given by[7]

$$E_{n,l,m} = -E_{n,l} + mB\mu_B, \tag{6.8}$$

where[8]

$$\mu_B = \frac{e\hbar}{2m_e}.$$

In Fig. 6.2 is shown the energy-level diagram for the five states with given n and $l = 2$, before and after the application of a magnetic field $\mathbf{B}$. We note that all the levels are equidistantly spaced, the energy difference between them being

$$\Delta E = \mu_B B.$$

Let us next consider the transition between a state with n_i, l_i, m_i and one with n_f, l_f, m_f. As an example we choose $l_i = 2$ and $l_f = 1$, so that the

[6] This was first clearly shown in the Stern–Gerlach experiment. W. Gerlach and O. Stern, Z. Physik **9**, 349 (192).

[7] The energy in the field is positive because the electron charge is taken as negative.

[8] m_e in this expression is the mass of the electron, not to be confused with the magnetic quantum number m.

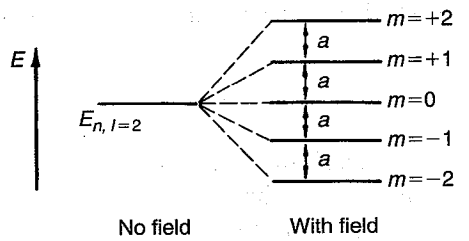

FIGURE 6.2 Splitting of an energy level under the influence of an external magnetic field. The level is assumed to have $l = 2$ and therefore is split into five equidistant sublevels.

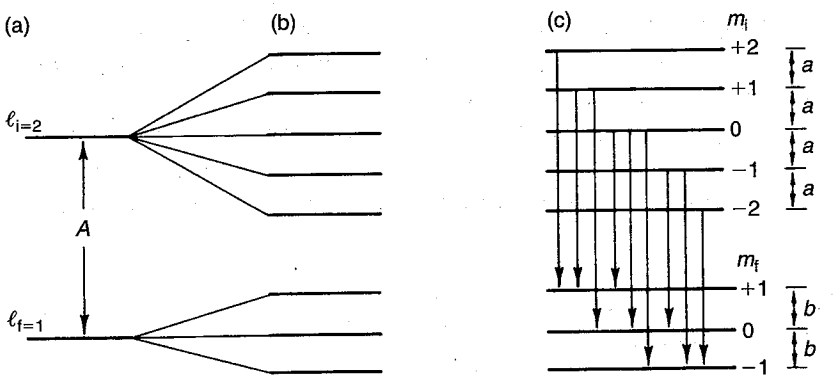

FIGURE 6.3 Splitting of a spectral line under the influence of an external magnetic field. (a) The initial level ($l = 2$) and the final level ($l = 1$) with no magnetic field are shown. A transition between these levels gives rise to the spectral lines. (b) The two levels after the magnetic field has been applied. (c) The nine allowed transitions between the eight sublevels of the initial and final states.

energy-level diagram is as shown in Fig. 6.3: without a magnetic field in Fig. 6.3a, and when the magnetic field is present in Fig. 6.3b.

However, for an *electric-dipole* transition to take place between two levels, certain selection rules must be fulfilled: in particular,

$$\Delta l = \pm 1. \tag{6.9}$$

Thus, when the field is turned on, we cannot expect transitions between the m sublevels with the same l, since they do not satisfy Eq. (6.9). Further, the transitions between the sublevels with $l_i = 2$ to the sublevels with

$l_f = 1$ that do satisfy Eq. (6.9) are now governed by the *additional* selection rule[9]

$$\Delta m = 0, \pm 1, \tag{6.10}$$

and thus only the transitions shown in Fig. 6.3c are allowed.

Let the energy splitting in the initial level be a, and in the final level be b, and let A be the energy difference between the two levels when no magnetic field is applied. Then the energy released in a transition $i \rightarrow f$ is given by

$$E_i - E_f = A_{if} + m_i a - m_f b. \tag{6.11}$$

These energy differences for the nine possible transitions shown in Fig. 6.3c are given in matrix form in Table 6.1; $\times$ indicates that the transition is forbidden and will not take place.

At this point the reader must be concerned about the use of a and b; according to our previous argument (Eq. (6.8)), as long as all levels are subject to the same magnetic field B, their splitting must also be the same, and

$$a = b = \mu_B B.$$

Thus, we see from Eq. (6.11) (or Table 6.1) that only *three* energy differences are possible

$$E_i - E_f = A + a(m_f - m_i) = A + a\Delta m,$$

where Δm is limited by the selection rule, Eq. (6.10), to the *three* values $+1, 0, -1$. Consequently, in the presence of a magnetic field B, the single

TABLE 6.1 Allowed Transitions from $l_i = 2$ to $l_f = 1$ and the Corresponding Energies

m of final state	m of initial state				
	$+2$	$+1$	0	-1	-2
$+1$	$A+2a-b$	$A+a-b$	$A-b$	$\times$	$\times$
0	$\times$	$A+a$	A	$A-a$	$\times$
-1	$\times$	$\times$	$A+b$	$A-a+b$	$A-2a+b$

[9]The selection rules of atomic spectroscopy are a consequence of the addition of angular momenta. In this specific case the selection rules indicate that we consider only *electric-dipole* radiation.

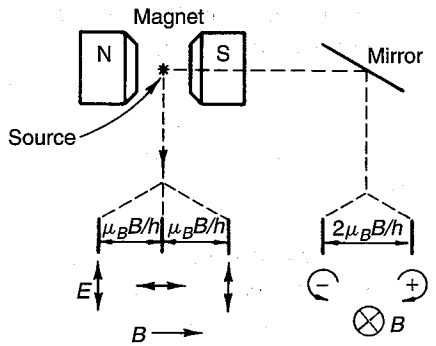

FIGURE 6.4 The polarization and separation of the components of a normal Zeeman multiplet when viewed in a direction normal to, and in a direction parallel to, the magnetic field.

spectral line of frequency $\nu = A/h$ is split into three components with frequencies

$$\nu_- = (A - \mu_B B)/h, \quad \nu_0 = A/h, \quad \text{and} \quad \nu_+ = (A + \mu_B B)/h$$

irrespective of the values of l_i and l_f. Furthermore, these spectral lines are polarized, as shown in Fig. 6.4. When the Zeeman effect is viewed in a direction *normal* to the axis of the magnetic field, the central component is polarized parallel to the axis, whereas the two outer ones are polarized normal to the axis of the field. When the Zeeman effect is observed *along* the axis of the field (by making a hole in the pole face, or using a mirror), only the two outer components appear, circularly polarized. The lines from $\Delta m = +1$ transitions appear with right-hand circular polarization, and from $\Delta m = -1$ transitions with left-hand circular polarization. The central line does not appear, since the electromagnetic field must always have the field vectors (**E** and **B**) normal to the direction of propagation.

The splitting of a spectral line into a triplet under the influence of a magnetic field is called the "*normal*" *Zeeman effect*, and is occasionally observed experimentally, as, for example, in the 579.0-nm line of mercury arising in a transition[10] from $^1D_2$ to $^1P_1$. However, in most cases the lines are split into more components, and even where a triplet appears it does not always show the spacing predicted by Eq. (6.8). This is due to the

[10]Note that both the initial and final states have $S = 0$.

intrinsic magnetic moment of the electron (associated with its spin) and will be discussed in the following sections.

6.2.2. The Influence of the Magnetic Moment of the Electron

In Section 1.6 it was discussed how the intrinsic angular momentum (spin) of the electrons **S** couples with the orbital angular momentum of the electrons **L** to give a resultant **J**; this coupling gave rise to the "fine structure" of the spectra.[11] The projections of **J** on the z axis are given by m_J, and we could expect (on the basis of our previous discussion) that the *total* magnetic moment of the electron will be given by

$$\boldsymbol{\mu} = \frac{\mu_B}{\hbar}\,\mathbf{J}. \tag{6.12}$$

Consequently, the energy-level splitting in a magnetic field B would be in analogy to Eq. (6.8):

$$\Delta E = -m_J \mu_B B. \tag{6.13}$$

These conclusions, however, are not correct because the *intrinsic* magnetic moment of the electron is related to the *intrinsic* angular momentum of the electron (the spin) through

$$\boldsymbol{\mu}_s = 2\,\frac{e}{2m_e}\,\mathbf{S} = 2\,\frac{e\hbar}{2m_e}\,s\mathbf{u}_s \tag{6.14}$$

and *not* according[12] to Eq. (6.6). Consequently, the *total* magnetic moment of the electron is given by the operator

$$\boldsymbol{\mu} = (\mu_B/\hbar)[\mathbf{L} + 2\mathbf{S}]. \tag{6.15}$$

[11] We will use the following notation: **L**, **S**, **J** represent angular momentum vectors that have magnitude $\hbar\sqrt{l(l+1)}$, $\hbar\sqrt{s(s+1)}$, $\hbar\sqrt{j(j+1)}$. The symbols l, j, etc. (s is always $s = \frac{1}{2}$), are the *quantum numbers* that label a one-electron state and appear in the above square root expressions. The symbols L, S, J, etc., are *quantum numbers* that label a state with more than one electron and are then used instead of l, s, j.

[12] The result of Eq. (6.14) is obtained in a natural way from the solution of the Dirac equation; it also emerges from the classical relativistic calculation of the "Thomas precession."

We can think of $\boldsymbol{\mu}$ as a vector oriented along **J** but of magnitude

$$\mu = \mu_B g\, J. \tag{6.16}$$

The numerical factor g is called the Landé g factor and a correct quantum-mechanical calculation gives[13]

$$g = 1 + \frac{j(j+1) + s(s+1) - l(l+1)}{2j(j+1)}. \tag{6.17}$$

The interesting consequence of Eqs. (6.16) and (6.17) is that now the splitting of a level due to an external field B is

$$E_{n,j,l,m_j} = -E_{n,j,l} + g\mu_B B m_j \tag{6.18}$$

and in contrast to Eq. (6.8) is *not* the same for all levels; it depends on the values of j and l of the level ($s = \frac{1}{2}$ always when one electron is considered). The sublevels are still equidistantly spaced but by an amount

$$\Delta E = g\mu_B B.$$

Consider then again the transitions between sublevels belonging to two states with different l (in order to satisfy Eq. (6.9)). However, since we are taking into account the electron spin, l is not a good quantum number, and instead the j values of the initial and final levels must be specified. If we

[13] This result can also be obtained from the vector model for the atomic electron. In Fig. 6.5 the three vectors **J**, **L**, and **S** are shown, and **L** and **S** couple into the resultant **J**, so that

$$\mathbf{J} = \mathbf{L} + \mathbf{S}.$$

By taking the squares of the vectors, we obtain the following values for the cosines

$$\cos(\mathbf{L}, \mathbf{J}) = \frac{j^2 + l^2 - s^2}{2lj} \qquad \cos(\mathbf{S}, \mathbf{J}) = \frac{j^2 + s^2 - l^2}{2sj}.$$

From Eq. (6.15) we see that

$$\mu/\mu_B = l\cos(\mathbf{L}, \mathbf{J}) + 2s\cos(\mathbf{S}, \mathbf{J}).$$

Thus

$$g = \frac{\mu}{\mu_B j} = \frac{j^2 + l^2 - s^2}{2j^2} + \frac{2j^2 + 2s^2 - 2l^2}{2j^2} = 1 + \frac{j^2 + s^2 - l^2}{2j^2}.$$

Finally we must replace j^2, s^2, and l^2 by their quantum-mechanical expectation values $j(j+1)$, etc., and we obtain Eq. (6.17).

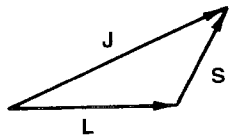

FIGURE 6.5 Addition of the orbital angular momentum **L** and of the spin angular momentum **S** into the total angular momentum **J**, according to the "vector model."

choose for this example $l_i = 1$ and $l_f = 0$, we have the choice of $j_i = \frac{3}{2}$ or $j_i = \frac{1}{2}$, whereas $j_f = \frac{1}{2}$. Transitions may occur only if they satisfy, in addition to Eq. (6.9), *also* the selection rules for j

$$\Delta j = 0\,,\ \pm 1 \qquad \text{not} \qquad j = 0 \rightarrow j = 0. \tag{6.9a}$$

Furthermore the selection rules for m_j must also be satisfied; they are the same as given by Eq. (6.10)

$$\Delta m_j = 0\,,\ \pm 1. \tag{6.10a}$$

In Fig. 6.6 the energy-level diagram is given without and with a magnetic field for the doublet initial state with $l = 1$, and the singlet final state, $l = 0$. Six possible transitions between the initial states with $j = \frac{3}{2}$ to the final state with $j = \frac{1}{2}$ are shown (as well as the four possible transitions from $j = \frac{1}{2}$ to $j = \frac{1}{2}$). By using Eq. (6.17) we obtain the following g factors

$$l = 1 \quad j = \tfrac{3}{2} \quad s = \tfrac{1}{2} \quad g = \tfrac{4}{3}$$
$$l = 1 \quad j = \tfrac{1}{2} \quad s = \tfrac{1}{2} \quad g = \tfrac{2}{3}$$
$$l = 0 \quad j = \tfrac{1}{2} \quad s = \tfrac{1}{2} \quad g = 2.$$

The sublevels in Fig. 6.6 have been spaced accordingly.

In Table 6.2 are listed the six transitions from $j = \frac{3}{2}$ to $j = \frac{1}{2}$ in analogy with Table 6.1. However, *since now* $a \neq b$, the spectral line is split into a six-component (symmetric) pattern. This structure of the spectral line is indicated in the lower part of Fig. 6.6; following adopted convention, the components with polarization parallel to the field are indicated above the base line, and with polarization normal to the field, below.[14] As before the parallel components have $\Delta m = 0$, the normal ones $\Delta m \pm 1$.

[14] It is also conventional to label the parallel components with π, and the normal ones by σ (from the German "Senkrecht").

TABLE 6.2 Allowed Transitions from $j_i = \frac{3}{2}$ to $j_f = \frac{1}{2}$ and the Corresponding Energies

m_j of final state	m_j of initial state $+\frac{3}{2}$	$+\frac{1}{2}$	$-\frac{1}{2}$	$-\frac{3}{2}$
$+\frac{1}{2}$	$A + \frac{3a}{2} - \frac{b}{2}$	$A + \frac{a}{2} - \frac{b}{2}$	$A - \frac{a}{2} - \frac{b}{2}$	×
$-\frac{1}{2}$	×	$A + \frac{a}{2} + \frac{b}{2}$	$A - \frac{a}{2} + \frac{b}{2}$	$A - \frac{3a}{2} + \frac{b}{2}$

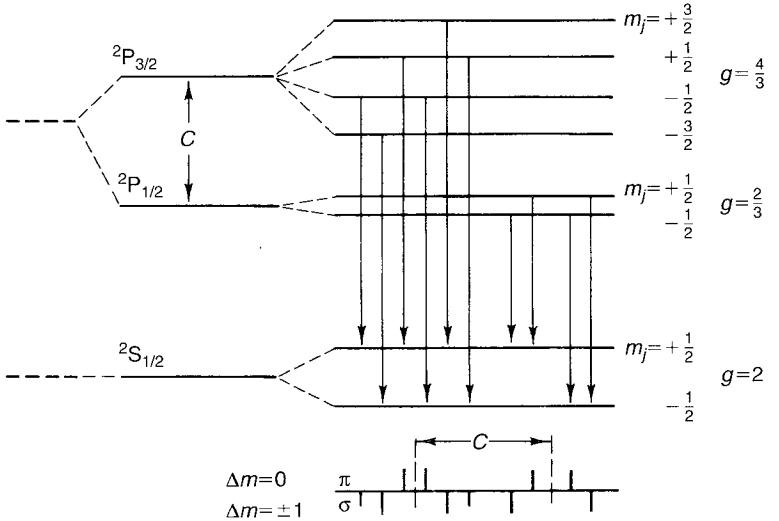

FIGURE 6.6 Energy levels of a single valence electron atom showing a P state and an S state. Due to the fine structure, the P state is split into a doublet with $j = \frac{3}{2}$ and $j = \frac{1}{2}$. Further, under the influence of an external magnetic field each of the three levels is split into sublevels as shown in the figure where account has been taken of the magnetic moment of the electron. The magnetic quantum number m_j for each sublevel is also shown as is the g factor for each level. The arrows indicate the allowed transitions between the initial and final states, and the structure of the line is shown in the lower part of the figure.

The horizontal spacing between the components is proportional to the differences in the energy of the transition, and the vertical height is proportional to the intensity of the components; the relative intensity can be predicted exactly since it involves only the comparison of matrix elements between the angular parts of the wave function.

As the magnetic field is raised, the separation of the components continues to increase linearly with the field until the separation between Zeeman components becomes on the order of the fine-structure separation (spacing C in Fig. 6.6). At this point the Zeeman components from the $j = \frac{3}{2} \rightarrow \frac{1}{2}$ and $j = \frac{1}{2} \rightarrow \frac{1}{2}$ transition begin to overlap; clearly the perturbation caused by the external magnetic field is on the order of the $\mathbf{L} \cdot \mathbf{S}$ energy and affects the coupling of $\mathbf{L}$ and $\mathbf{S}$ into $\mathbf{J}$; $\mathbf{J}$ ceases to be a "good quantum number."

For very strong fields, $\mathbf{L}$ and $\mathbf{S}$ become completely uncoupled, so that the orbital and intrinsic magnetic moments of the electron interact with the field independently, giving rise to an energy shift

$$\begin{aligned}\Delta E &= -\frac{\mu_B}{\hbar}\mathbf{L}\cdot B - 2\frac{\mu_B}{\hbar}\mathbf{S}\cdot\mathbf{B} - a\mathbf{L}\cdot\mathbf{S} \\ &= -\mu_B B(m_l + 2m_s) - a m_l m_s. \end{aligned} \tag{6.19}$$

In this region one speaks of the Pashen–Back effect. The reader can find more details in the references, in particular in the classic text by Condon and Shortley.

So far we have discussed the case where the atom has only a single valence electron. In Section 1.6 we considered also atoms with two valence electrons and saw that for Hg the total angular momentum $\mathbf{J} = \mathbf{L}+\mathbf{S}$, where $\mathbf{L}$ results from the coupling of $\boldsymbol{l}_1$ and $\boldsymbol{l}_2$ and $\mathbf{S}$ from the coupling of $\boldsymbol{s}_1$ and $\boldsymbol{s}_2$. In this case the g factor is still given by Eq. (6.17), but by using L, S, and J, the quantum numbers for the coupled angular momenta.

An interesting case arises in the 579.07-nm yellow line of Hg, which is due to the transition from the $6\,{}^1D_2$ state to the $6\,{}^1P_1$ state. (See Fig. 1.24 for the energy level diagram of Hg.) As the reader should verify, by using Eq. (6.17), the g factors of the initial and final state are both equal to 1. Thus we have exactly the situation shown in Fig. 6.3, and the line splits into three components (normal Zeeman effect).

6.3. HYPERFINE STRUCTURE

Spectral lines, when examined under high resolution, do show structure even in the absence of an external magnetic field. As already mentioned this *hyperfine* structure arises from the interaction of the atomic electrons with the nucleus. The largest effect arises from the magnetic-dipole moment of the nucleus, but the effect of higher order moments are also observed. A related effect is the isotope shift, which shifts the spectral lines between isotopes, i.e., atoms of the same element but with nuclei of different mass.

6.3.1. The Effects of Nuclear Spin

Nuclei can have an intrinsic angular momentum (spin) different from 0. We use $\mathbf{I}$ to designate the nuclear spin which can take the values (i.e., the quantum number) $0, \frac{1}{2}, 1, \frac{3}{2}, \ldots$ that can reach very high values for excited nuclear states. When $I \geq \frac{1}{2}$ we can expect that the "spinning" charge of the nucleus will give rise to a magnetic moment (see Eq. (6.6)) oriented along the spin axis

$$\boldsymbol{\mu} = -\frac{e}{2M}\mathbf{I},$$

where M is the mass of the nucleus. In addition, nuclei exhibit an intrinsic magnetization,[15] so that in general we have

$$\boldsymbol{\mu} = -g_I \frac{e}{2m_p}\mathbf{I} = g_I \mu_N I \mathbf{u}_I,$$

where $\mathbf{u}_I$ is a unit vector along the spin direction, and

$$\mu_N = \frac{e\hbar}{2m_p}$$

is the *nuclear magneton*; m_p is the proton mass. The numerical factor g_I includes all the effects of intrinsic and orbital magnetization of the nucleus and can be obtained only from a theory of nuclear structure.

The magnetic moment of the nucleus, $\boldsymbol{\mu}$, will interact with the magnetic field $\mathbf{B}_e(0)$ produced by the atomic electrons (at the nucleus; Fig. 6.7). This interaction then results in a shift of the energy levels of the atom by the amount

$$\Delta E = -\boldsymbol{\mu}\cdot\mathbf{B}_e(0). \tag{6.20}$$

The direction of $\mathbf{B}_e(0)$ is that given by the total angular momentum of the atomic electrons, namely,[16] $\mathbf{J}$, so that

$$\Delta E = +\left(\frac{\mu}{|I|}\right)\left(\frac{B_e(0)}{|J|}\right)\mathbf{I}\cdot\mathbf{J}. \tag{6.21}$$

[15] This gives rise to the so-called "anomalous" magnetic moment of the nucleon; for example, the neutron (an uncharged particle) has a magnetic moment of $-1.91\,\mu_N$.

[16] The direction of $\mathbf{B}_e(0)$ is really opposite to $\mathbf{J}$ because the electron has negative charge.

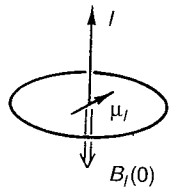

FIGURE 6.7 Interaction of the nuclear magnetic moment with the magnetic field produced by the electrons at the nucleus.

Thus, we expect the splitting of a level of given J according to the possible values of $(\mathbf{I} \cdot \mathbf{J})$, which, as we know, are quantized. The situation is analogous to that of the fine structure, where the interaction was proportional to the $(\mathbf{L} \cdot \mathbf{S})$ term. In that instance the two angular momenta coupled into a resultant $\mathbf{J} = (\mathbf{L} + \mathbf{S})$ according to the quantum-mechanical laws of addition of angular momentum. In the present situation, $\mathbf{J}$ and $\mathbf{I}$ couple into a total angular momentum of the atom designated by $\mathbf{F}$:

$$\mathbf{F} = (\mathbf{I} + \mathbf{J}). \tag{6.22}$$

An energy level of given $\mathbf{J}$ is then split into sublevels having all possible values of F, namely, the integers (or half-integers)

$$|J - I| \leq F \leq |J + I|.$$

Thus if $I = \frac{1}{2}$, the level is split into two components, with $F_1 = J + \frac{1}{2}$ and $F_2 = J - \frac{1}{2}$ (provided $J \geq \frac{1}{2}$); if $I = 1$, the level is split into three components with $F_1 = J - 1$, $F_2 = J$, and $F_3 = J + 1$ (provided $J \geq 1$); etc. This situation is shown in Fig. 6.8, and we see that if J is known, the number of hyperfine structure components of a spectral line provides direct information on the spin of the nucleus.

If either $I = 0$ or $J = 0$, no splitting of the energy levels can occur since the interaction energy specified by Eq. (6.21) vanishes. This is to be expected because if $I = 0$, the nucleus cannot have a dipole moment, and if $J = 0$, then by symmetry, the magnetic field at the origin $B_e(0) = 0$.

Using Eq. (6.22), we can now obtain the expectation value of the operator $(\mathbf{I} \cdot \mathbf{J})$ that appears in Eq. (6.21); referring to the vector model

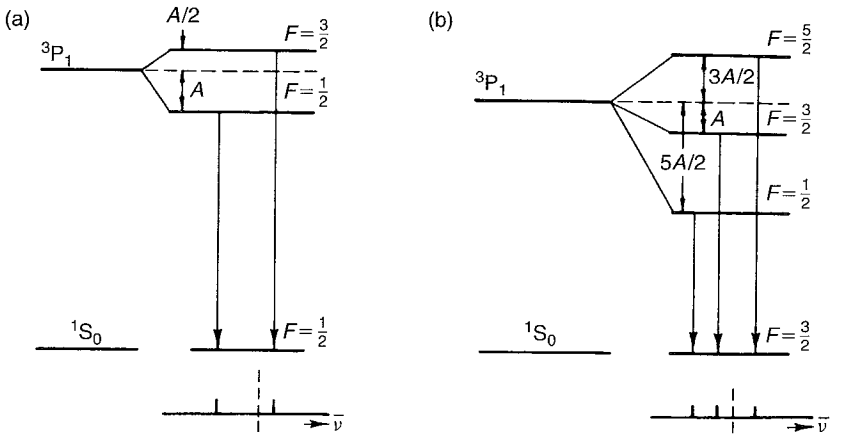

FIGURE 6.8 Hyperfine structure splitting of a $^3P_1$ atomic energy level, and the allowed transitions between the hyperfine structure components of this level and a $^1S_0$ final state when the spin of the nucleus is (a) $I = \frac{1}{2}$ and (b) $I = \frac{3}{2}$.

we write "classically"

$$\cos(\mathbf{I}, \mathbf{J}) = \frac{F^2 - I^2 - J^2}{2IJ}$$

and replacing F^2, etc., by the quantum-mechanical expectation values $F(F+1)$ we obtain

$$\Delta E = \frac{A}{2}[F(F+1) - I(I+1) - J(J+1)], \tag{6.23}$$

where the constant A is given by

$$A = \frac{\mu}{|I|} \frac{\langle B_e(0) \rangle}{|J|}. \tag{6.24}$$

Note that the energy splitting between sublevels, as given by Eq. (6.23) (and shown in Fig. 6.8), is not symmetric. Further, if we succeed in extracting from the experimental data the constant A, we can obtain the nuclear magnetic moment if $\langle B_e(0) \rangle$ is known.

The calculation of the average value of the magnetic field of the electrons at the nucleus $\langle B_e(0) \rangle$, however, is not easy to perform, and depends on the orbital angular momentum of the valence electron or electrons. Expressions

for the "constant" A in terms of the atomic wave function can be found in the references (see Kopferman).

6.3.2. Isotope Shift

Figure 6.9 shows the hyperfine structure of the 253.7-nm line of *natural* mercury when examined under high resolution. When the lines are correctly identified we note that the different isotopes have different energies. Indeed natural mercury consists of several isotopes with the abundances shown in Table 6.3; the nuclear spin, nuclear-dipole magnetic moment, and electric-quadrupole moment are also indicated.

The isotope shift arises from two effects: (a) The finite mass of the nucleus: The nucleus is much heavier than the electron, but we can consider its mass as infinite only to a first approximation. (b) The finite size of the nucleus: The nuclear radius is much smaller than the orbit of the electron, but we can consider the nucleus as a point only to a first-order approximation. For light elements the isotope shift is mainly due to the effect of the finite mass, whereas for the heavy elements it is mainly due to the finite size effect. It should also be evident that we cannot measure the shift in the energy level of a single isotope, but only the difference in the shift between two or more isotopes. This is shown in Fig. 6.10a.

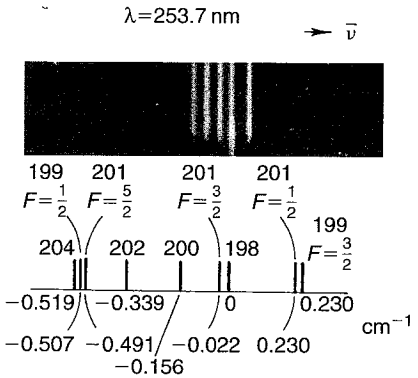

FIGURE 6.9 High-resolution spectrogram of the 253.7-nm line of natural mercury. In the lower part of the figure the various components are identified and their separation from the position of the ^{198}Hg component is also indicated. (Note that the ^{198}Hg component appears in the spectrogram as the longer line.)

TABLE 6.3 Properties of the Isotopes of Natural Hg ($Z = 80$)

Isotope	Abundance (percent)	N (neutrons)	I (nuclear spin)	μ (units of μ_N)	Q ($\text{cm}^2 \times 10^{-24}$)
198	10.1	118	0	0	
199	17.0	119	$\frac{1}{2}$	0.876	
200	23.2	120	0	0	
201	13.2	121	$\frac{3}{2}$	−0.723	0.38
202	29.6	122	0	0	
204	6.7	124	0	0	

In terms of the solutions of the Schrödinger equation we must consider both the electron and nucleus as revolving about the *center of mass* of the electron–nucleus system. This leads back to the Schrödinger equation for a stationary attractive center (nucleus) if the mass of the electron is replaced by its *reduced mass*

$$m' = m_e \frac{M}{M + m_e}, \tag{6.25}$$

where M is the mass of the nucleus. Then the energy of a hydrogen-like level is given by

$$E_n = -\frac{hcR_\infty Z^2}{n^2}\left(\frac{M}{M + m_e}\right) \simeq -\frac{hcR_\infty Z^2}{n^2}\left(1 - \frac{m_e}{M}\right) \tag{6.26}$$

where Z is the nuclear charge. For instance, the value of the Rydberg as obtained from the spectra of hydrogen and deuterium will differ by

$$\frac{R_\text{H}}{R_\text{D}} \simeq \left(1 - \frac{m_e}{2m_p}\right), \tag{6.27}$$

where we set the mass of the deuteron $m_d \sim 2m_p$. This will shift the spectral lines by 3×10^{-4}, which we can observe in the laboratory.

For the heavier elements the isotope shift due to finite mass becomes very small. Instead it is the finite size of the nucleus that is the dominant reason for a shift of the energy levels. Consider Fig. 6.10b where curve (a) represents the Coulomb potential of a point charge. If it is assumed that the electric charge of the nucleus is distributed on a spherical surface of radius r_0, then the potential will not diverge at $r = 0$, but will be constant for all $r \leq r_0$. Thus the potential seen by an electron will be of the form shown